Exploring Celestial Cartography: Assessing Precision in Asteroid Vesta Localization with MTSU's 16" Schmidt-Cassegrain Telescope

Ahmeed Yinusa, Dipesh Shrestha, Isaac Shirk, Momina Liaqat Ali, Nada Srour, Thuan Nhan, Yuan Chen

March 2024

1 Introduction

Celestial cartography, the practice of mapping the sky, is a fundamental tool for uncovering the universe's mysteries. It allows astronomers to investigate the positions and movements of celestial objects, revealing information about their nature and behavior. The MTSU's 16" Schmidt-Cassegrain Telescope was used in this study to investigate the precision of celestial object localization, with a specific focus on the asteroid Vesta.

Vesta, one of the largest asteroids in the asteroid belt between Mars and Jupiter, provides insight into the early stages of our solar system's development. Studying Vesta can disclose important details regarding its composition, history, and function in the solar system's dynamics. Using the capabilities of the MTSU observatory complex, which includes a 16" Schmidt-Cassegrain telescope outfitted with a CCD camera, this study describes the process of obtaining detailed photographs of Vesta and properly estimating its position in the night sky.

Observations for this study were conducted on March 13, 2024, between 8 and 9 p.m. local time in Murfreesboro, TN. By assessing the precision of Vesta's localization during this observation period, our goal was to investigate the capabilities of the MTSU's telescope in accurately determining the positions of celestial objects, thus enhancing our understanding of the instrument's performance in celestial mapping and contributing to the advancement of astronomical research.

2 Problem Statement

The accurate location of celestial objects is critical for many astronomical investigations, including tracking asteroids and comets and comprehending galaxies'

motions. However, establishing accurate localization can be difficult due to air distortion, instrument constraints, and observational errors. To increase our understanding of the universe, We need to evaluate the precision of localization techniques applied to images captured by devices such as MTSU's telescope.

3 Objective

This study aims to assess the accuracy of celestial object localization with a specific emphasis on the asteroid Vesta, utilizing the 16" Schmidt-Cassegrain telescope at Middle Tennessee State University (MTSU). By taking detailed photographs of Vesta and pinpointing its location in the night sky, our objective is to examine the telescope's ability to properly determine the positions of celestial objects and to contribute to the advancement of astronomical research.

4 Methodology

Using the MTSU observatory as it is currently configured, two sets of images (.fit files) of the asteroid Vesta are taken. The first sets of images contain 8 images of 30 second exposures of the area around the asteroid Vesta. Images were taken about every three minutes. The second sets of images contains 9 images of 10 second exposures of the area around the asteroid Vesta. These images were taken in five minute intervals approximately. Our goal is to determine if the 16" Schmidt-Cassegrain Telescope at MTSU can accurately measure the position of an astronomical object in a star field and thus be used to measure the stellar parallax of stars.

4.1 Using Astrometry.net and twirl library

4.1.1 Data Acquisition and Preprocessing:

We employed preprocessing steps to modify the images based on distortions, such as flat-field correction, dark frame subtraction, and bias subtraction from the raw data. After preprocessing, images were analyzed in Python using the "*astropy*"[1] library to read the FITS files and extract the metadata information. We developed a metadata summary table for each image involving the file name, DATE-OBS, Julian Date, RA, DEC, Width, and Height.

4.1.2 Star Detection and Photometry:

The star detection procedure for these images was performed employing the '*DAOStarFinder*' algorithm of the '*photutils*'[6] python library package that detected point sources as possible and potential star candidates. The algorithm's parameters, including *full width at half maximum (FWHM)* and *threshold*, were varied and optimized to achieve maximal detection of stars and a minimal number of false positives from noise and background fluctuations. For each detected

source, we determined the *centroid coordinates* and photometric measurements: (*flux* and *apparent magnitude*).

4.1.3 WCS Calibration:

We implemented the World Coordinate System (WCS)[2] calibration on the images to convert (*map*) pixel coordinates to sky (celestial) coordinates (RA and DEC). For this project, the procedure for the calibration comprises two major stages. Firstly, the initial WCS solutions were achieved using the '*Astrometry.net*[7]' service via a Python library called "*astroquery*,"[3] which gave a transformation matrix for every image. This output solution contained TAN (*tangential*) projection with the parameters CRVAL1, CRVAL2 (RA and DEC of the reference point), CRPIX1, CRPIX2 (reference pixel), and CD elements of a matrix (coefficients of the transformation matrix).

Secondly, we utilized the "*twirl library*"[4] to generate WCS from querying the *Gaia catalog* to develop an alternative WCS solution to the first procedure. This process was employed to facilitate the comparison of calibration accuracy with '*Astrometry.net*[7]' using the "*astroquery*,"[3] Python library.

4.1.4 Gaia Catalog Overlay:

To ensure and validate the accuracy of the WCS calibration, we superimposed stars from the Gaia catalog [5] on our images. This step consisted of associating the cataloged sky (*celestial coordinates*) for the Gaia stars with the WCS-calibrated pixel coordinates of our detected sources. Deviation of superimposed overlaid catalog star positions from the detected sources was an indicator of calibration accuracy. We repeated the overlay process for WCS solutions with and without SIP corrections.

4.1.5 Data Analysis:

We determined the calibration accuracy by simply developing visual inspections of the overlays of the Gaia catalog [5] stars on the images. Positional offsets between the catalog positions and the detected star centroids were computed for quantitative evaluation. At first, the WCS calibration without SIP corrections was examined. We further evaluated the effect of optical distortion corrections by analyzing the SIP-calibrated images. It was observed that the WCS solutions without SIP corrections introduced a constant systematic error toward the images' edges. However, when SIP corrections were applied, the overlays significantly improved alignment accuracy throughout the field. The essential role and success of SIP corrections for high-quality astrometric analysis were demonstrated by comparing the WCS calibrations.

4.2 Using Manual Calibration of detected Stars

4.2.1 Image Processing

Each acquired FITS file is preprocessed to enhance the quality of the data and facilitate accurate analysis:

1. **Background Subtraction**: The acquired images often contain background noise caused by various factors such as electronic noise, thermal noise, and light pollution. Background subtraction aims to remove this noise, allowing for clearer identification of celestial objects.

2. **Star Detection**: Once the background is subtracted, `DAOStarfinder` from `photutils` library [6] is used to locate stars within the image. Then we analyze the intensity of each identified stars and retained the positions of 14 brightest celestial objects that includes vesta and 13 reference stars. After finding these positions of reference stars in one image, same values with calculated offset is utilized for all other images.

3. **Centroid Determination for the Brightest Stars**: After star detection, the centroids (geometric centers) of the brightest stars in the image are determined. For that, image is cropped around approximate location of star ensuring to include the entire star. Then we utilized texttttOpenCV library [8] to find exact centroid within a cropped region of an image, using contour detection and moment calculations. The centroids of bright stars serve as key reference points for subsequent calibration and analysis steps.

These preprocessing steps are essential for preparing the raw image data for further analysis, ensuring accurate measurements and reliable results.

4.2.2 WCS Calibration

A crucial step in the analysis involves calibrating a World Coordinate System (WCS) using the positions of reference stars. This calibration allows for the conversion of pixel coordinates to celestial coordinates (Right Ascension, RA, and Declination, Dec). The WCS calibration is based on the following primary equations:

$$\Delta RA = RA - CRVAL_1 = CD1_1 \cdot (x - CRPIX_1) + CD1_2 \cdot (y - CRPIX_2) \tag{1}$$

$$\Delta Dec = Dec - CRVAL_2 = CD2_1 \cdot (x - CRPIX_1) + CD2_2 \cdot (y - CRPIX_2) \tag{2}$$

Where:

- RA and Dec represent the celestial coordinates of the stars,

- $CRVAL_1$ and $CRVAL_2$ denote the celestial coordinates of the reference pixel for Right Ascension and Declination, respectively,
- $CD1_1$, $CD1_2$, $CD2_1$, and $CD2_2$ are elements of the CD matrix that convert pixel coordinates to celestial coordinates,
- x and y denote the pixel coordinates,
- $CRPIX_1$ and $CRPIX_2$ represent the reference pixel coordinates for the x and y axes, respectively.

By solving these equations, we obtain the transformation matrix (CD matrix) necessary for accurate WCS calibration. We utilize the known positions of reference stars, that we obtained from Gaia archive [5] manually, to solve these equations.

4.2.3 Position Determination

Utilizing the calibrated WCS, pixel coordinates of Vesta are converted to celestial coordinates (RA and Dec). The calculated coordinates are compared with the actual known positions of Vesta.

4.2.4 Error Analysis

Errors between the calculated and actual positions of Vesta are computed. Average errors in both RA and Dec are analyzed to evaluate the accuracy of the telescope's measurements. Further, the model is also compared with the performance of models from other methodologies by evaluating error on locating several stars.

4.3 Fixing CD matrix with astrometry.net

4.3.1 Estimating Vesta Position

To estimate the position of Vesta by fixing CD matrix with astrometry.net, we performed a few simple steps which are listed below:

- Background Subtraction: We employed median background estimator and sigma clipped statistics to subtract background from the images.
- Contrast Enhancement: Histogram equalization is used to increase the image contrast, which makes features (stars) more visible.
- Detect Stars: We further used DOAStarFinder algorithm to carry-out star detection process. DOAStarFinder is robust in calculating the star threshold with the help of standard deviation of the image for which we already subtracted the background.
- Circular Apertures: It adds circular apertures on identified stars and presents the original image with increased contrast.

- Locating Vesta: We highlighted the objects in the list based in their index and located vesta using stellarium by comparing the positions of stars near Vesta in the provided images and with stellarium. Then once we located Vesta, we computed its pixels using the centroid information.

4.3.2 Fixing CD matrix

4.3.3 Obtaining WCS value from astrometry.net

In this step, we acquired crucial calibration data for our FITS (Flexible Image Transport System) files by utilizing the astrometry.net web inteface. After processing each .fit file, Astrometry.net gives us the pixel values and Celestial Distortion (CD) matrix required for precise astrometric calibration.

4.3.4 Error Analysis Process

To ensure the accuracy of our calibration, we conducted a meticulous error analysis. Initially, we submitted the first .fit file to astrometry.net and compared the Right Ascension (RA) and Declination (DEC) values derived from the astrometry.net solution with those from the Gaia Catalog at the specific time of observation. This comparison allowed us to compute the initial error for this first image.

Subsequently, we repeated this process for the last image taken at the same exposure setting on that day. By "last image," we refer to the final image captured at that exposure duration. Once again, we compared the astrometry.net-derived RA and DEC values with those from the Gaia Catalog and computed the error. This comprehensive approach ensured we accounted for potential variations or drift in the telescope's alignment or tracking throughout the observation session.

5 Results

5.1 Using Astrometry.net and twirl library

This research section explains the results of the *Astronometry.net*[7] and *twirl Python library*[4] approaches in tracking the positions of the vesta in the images.

5.1.1 30 and 10 Time Exposures

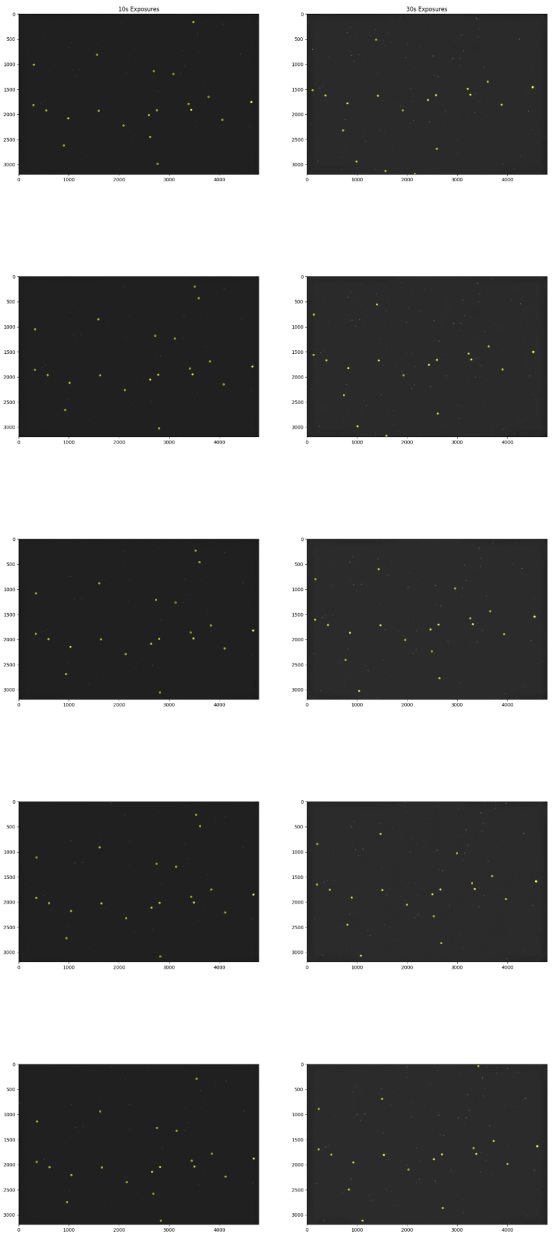

Figure 1: 30 and 10 Time Exposures of Vesta

Figure 1 depicts the evaluation of astrometric calibration techniques by displaying ten astronomical images corresponding to two exposures: *10 and 30 seconds*. The figures are annotated with yellow-marked posts to show the deviations (*errors*) observed between the positions of the detected stars and the celestial coordinates from the Gaia catalog data. Moreover, the 10s exposure panel shows the central clustering of the markers that become dispersed towards the periphery, a characteristic of a distortion-sensitive calibration technique. However, the panel for the 30-second exposure shows decreased dispersion of markers, thereby reflecting a higher calibration accuracy, probably attributable to an enhancement in the Signal-to-Noise ratio (S/N).

In general, this visualization emphasizes the impact of the exposure time on astrometric precision and the necessity of corrective measures. In this procedure, the SIP minimizes the effects of optical distortion in the calibration of the images. Though these inconsistencies are observed, the repetition of the star field in the pictures merely proves that the viewing procedure is stable.

Comparing these two types of exposures indicates the importance of enhancing the calibration techniques in astrophotometry. Such an improvement will ensure that future scientific research, e.g., asteroid motion tracking and precise photometric experiments, will be based on the correct position data.

5.1.2 Gaia Stars Overlayed and Twirl WCS for the First Five Images per Exposure Length

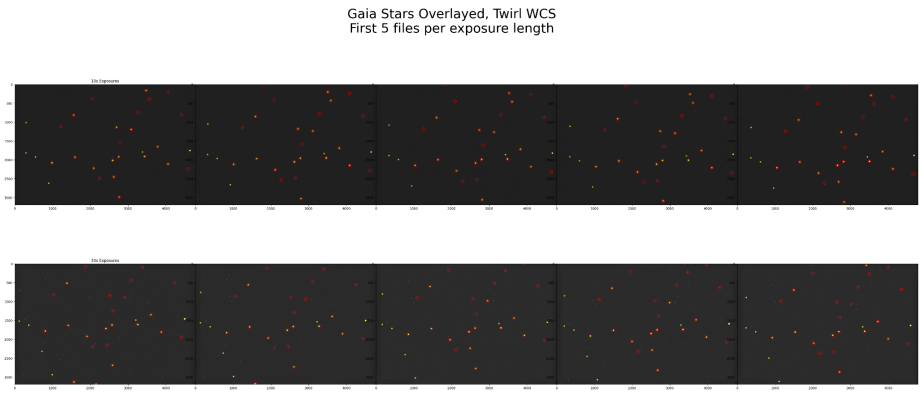

Figure 2: Gaia Stars Overlayed and Twirl WCS

Figure 2 demonstrates the astrometric calibration of a sequence of astronomical images by the Twirl World Coordinate System (WCS). Ten panels represent the first five images from two sets of exposures: 10 s (top) and 30 s (bottom). The yellow points on each image mark the stars detected in the image, and the red circles denote their expected locations as per the Gaia catalog, serving as a direct comparison for the calibration precision.

In the overlays, a high degree of alignment between the detected positions and catalog data is observed, which suggests an efficient calibration with the Twirl WCS method. Although near-perfect overlaps are more common in the middle of the images, some offsets are apparent, especially close to the edge, which indicates areas where the calibration may be improved.

5.1.3 Gaia Stars Overlayed and Astro WCS with SIP for the First Five Images per Exposure Length

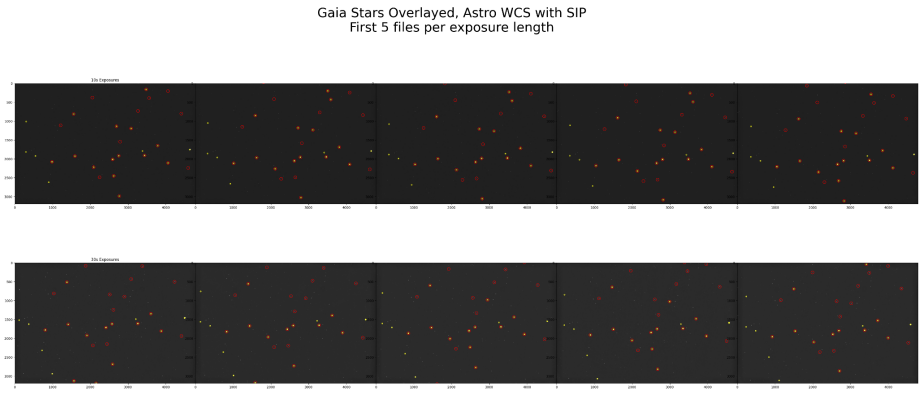

Figure 3: Gaia Stars Overlayed and Astro WCS with SIP

Figure 3 shows the astrometric calibration of two astronomical images using WCS with the SIP Astrometry.net corrections. The upper panel illustrates five frames of 10-second exposure, whereas the lower panel depicts the same 30-second exposure. The yellow points show the detected stars and the calibrated WCS with SIP has adjusted the Gaia catalog predictions in the form of red circles.

The precision of the calibration is evident from the alignment of the detected star positions (yellow points) and the Gaia catalog[5] overlays (red circles). The high correlation between these points, especially in the 10s exposure, confirms effective calibration, which reduces optical distortions. In the 30s exposures, while more light is collected, the retained accuracy of the SIP-corrected WCS overlays implies stable calibration across different exposure durations.

5.1.4 Gaia Stars Overlayed and Astro WCS without SIP for the First Five Images per Exposure Length

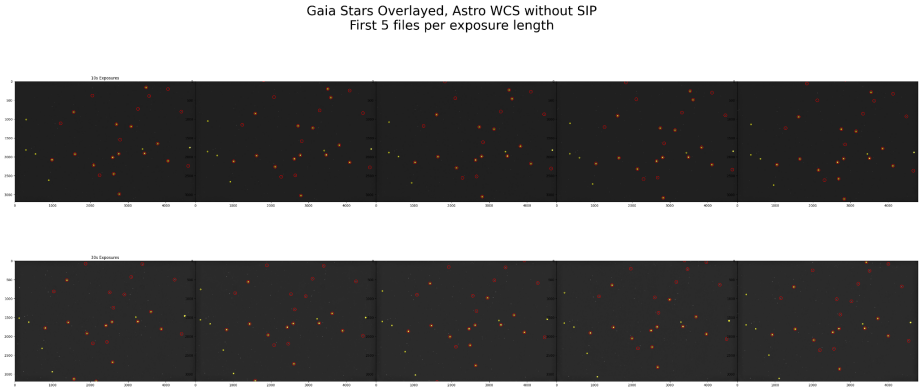

Figure 4: Gaia Stars Overlayed and Astro WCS without SIP

Figure 4 shows the astrometric calibrations conducted by Astrometry.net WCS with no Simple Imaging Polynomial (SIP) corrections. The figure is divided into two panels featuring five images of ten-second and 30-second exposures.

The yellow markers indicate stars found in the images, and the red circles are overlaid to show the expected positions according to the Gaia star catalog. Differences in the markers and circles show errors in the WCS calibration process. The unused SIP correction is more visible, especially on the image edges, where optical distortions usually cause position inaccuracy on celestial objects.

5.2 Using Manual Calibration of detected Stars

The results of our analysis, using manual calibration of detected stars, are presented in this section.

5.2.1 Locating Stars

Figure 5 illustrates the positions of Vesta and reference stars in the star field, as detected by the MTSU's Schmidt-Cassegrain Telescope. Additionally, Figure 6 shows how the centroid position of a celestial object is improved through process of finding real centroid. It displays both the approximate location of centroid and the actual centroid determination.

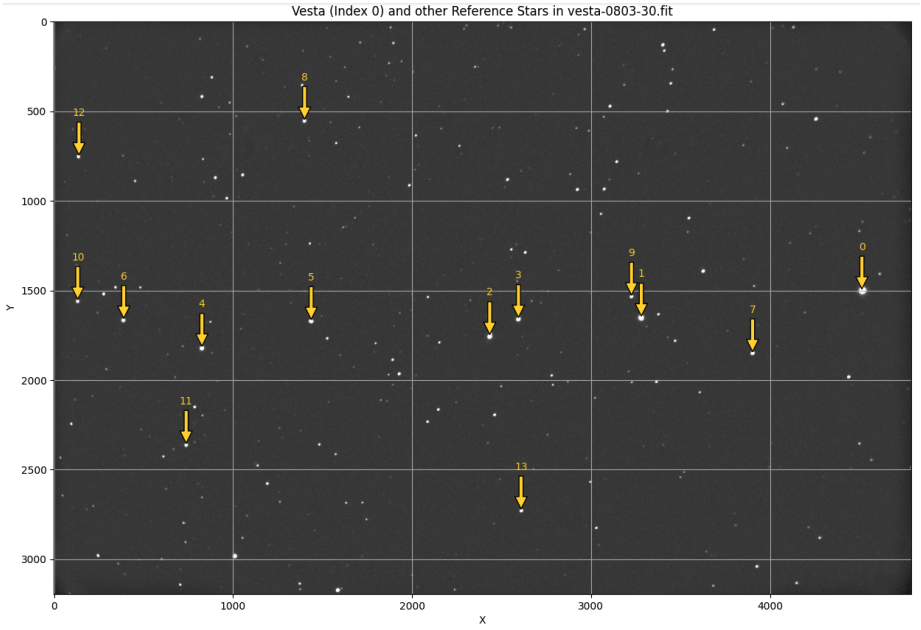

Figure 5: Locating Vesta and reference stars positions

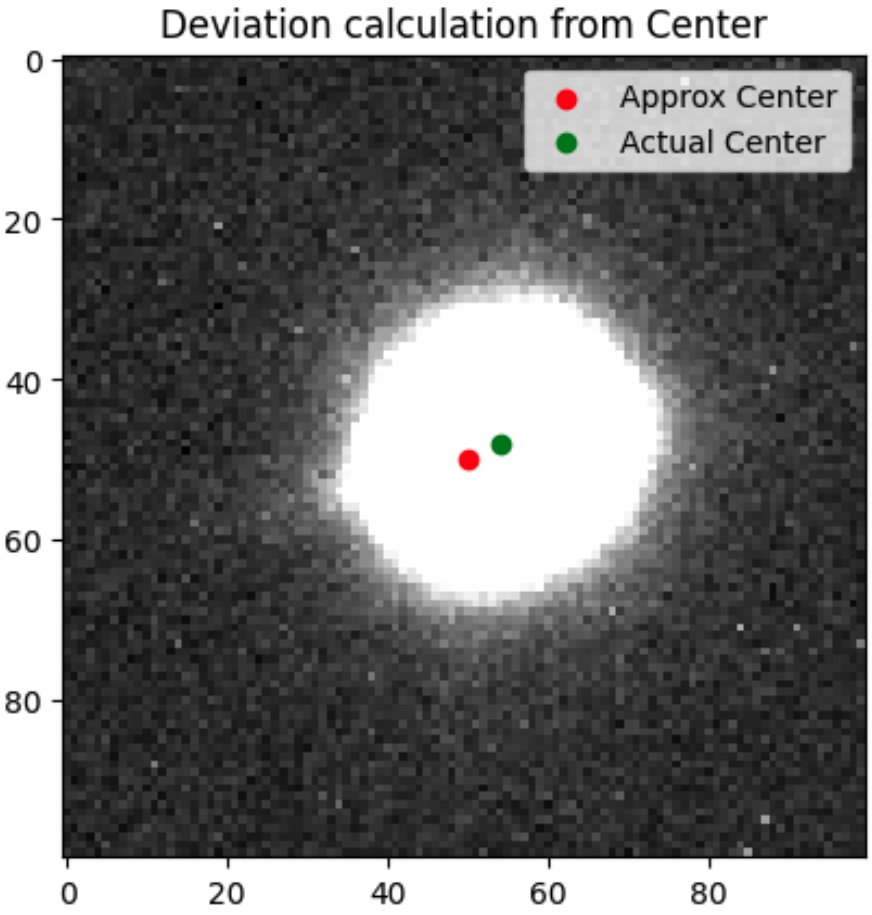

Figure 6: Finding the real centroid

Furthermore, Figure 7 depicts the alignment of the image overlayed by the real RA/Dec positions of stars, which were converted to x, y locations using calculated CD matrices.

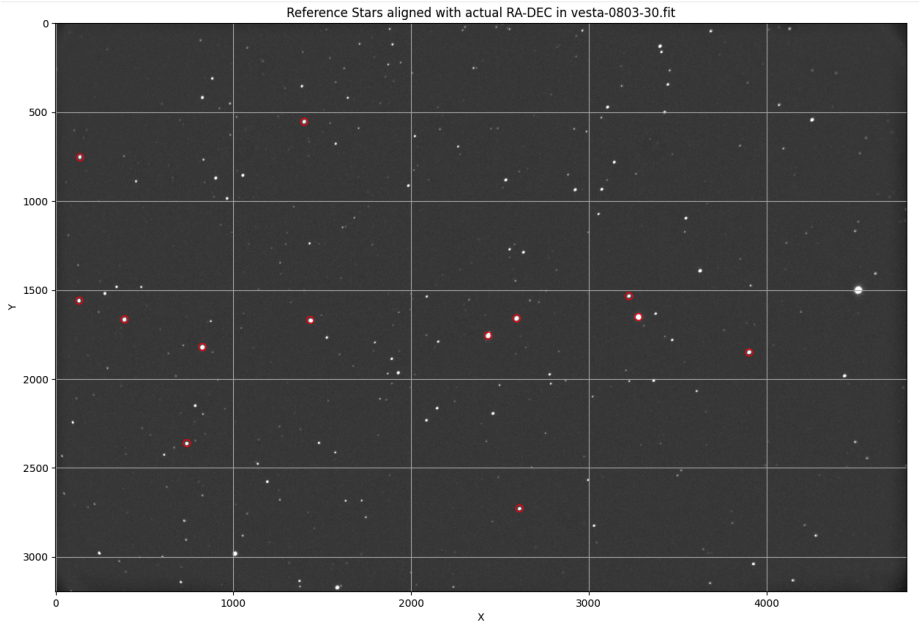

Figure 7: Alignment of real RA/Dec positions with image

5.2.2 Evaluation of Vesta's Motion

We evaluated Vesta's motion in the night sky for both 10-second and 30-second exposure images. The calculated errors in RA and DEC for the two exposure times are summarized below:

Figure 8 and Figure 9 show the real and calculated positions of Vesta for 10-second and 30-second exposures, respectively.

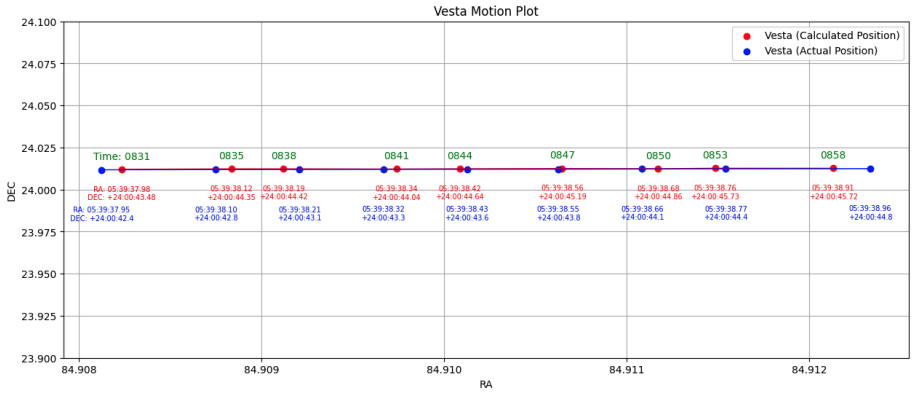

Figure 8: Real and calculated positions of Vesta for 10-second exposure

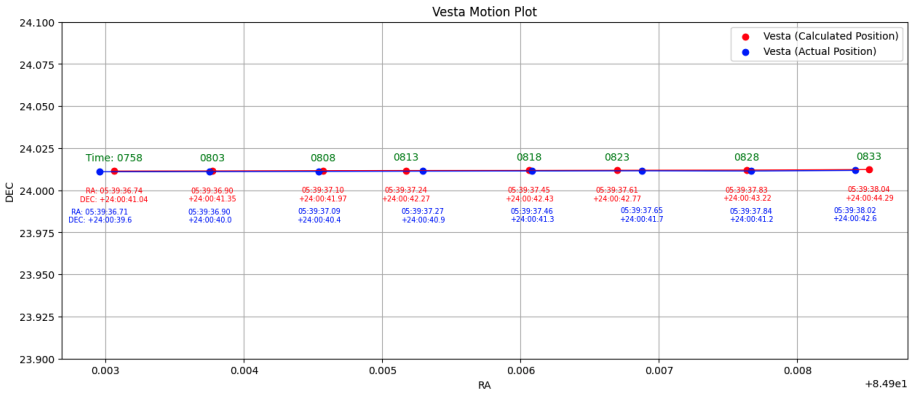

Figure 9: Real and calculated positions of Vesta for 30-second exposure

For 10-second exposure:

- Average RA error: 2.04×10^{-2} arcsec
- Average DEC error: 1.13×10^{0} arcsec

For 30-second exposure:

- Average RA error: 1.82×10^{-2} arcsec
- Average DEC error: 1.45×10^{0} arcsec

The results indicate that the errors in both RA and DEC are within acceptable limits for both exposure times, confirming the reliability of our measurements.

5.3 Fixing CD matrix with astrometry.net

Having identified the errors for the first and last images, we proceeded to adjust the CD matrix. CD matrix is a 2x2 matrix which is shown in Eq 3:

$$\begin{pmatrix} CD[0][0] & CD[0][1] \\ CD[1][0] & CD[1][1] \end{pmatrix} \tag{3}$$

By subtracting 0.0000101 from CD[0][0] and 0.00000019 from CD[1][0] for images recorded at exposure 30 and for exposure 10 images we subtracted 0.00001 and 0.0000001 from CD[0][0] and CD[1][0] respectively. This adjustment compensated for the observed errors which can be considered as a starting point to identify the motion of Vesta although this approach is not very accurate but it follows the trend of Vesta motion over a period of time, ensuring that the CD matrix may reflect the true astrometric characteristics of the telescope and

camera system. Importantly, we applied the same error correction to all images captured at the same exposure duration on that day. This standardized approach helped maintain consistency across our entire dataset, facilitating precise astrometric calibration for each image. Figure 10 and Figure 11 illustrates the results obtained with this approach.

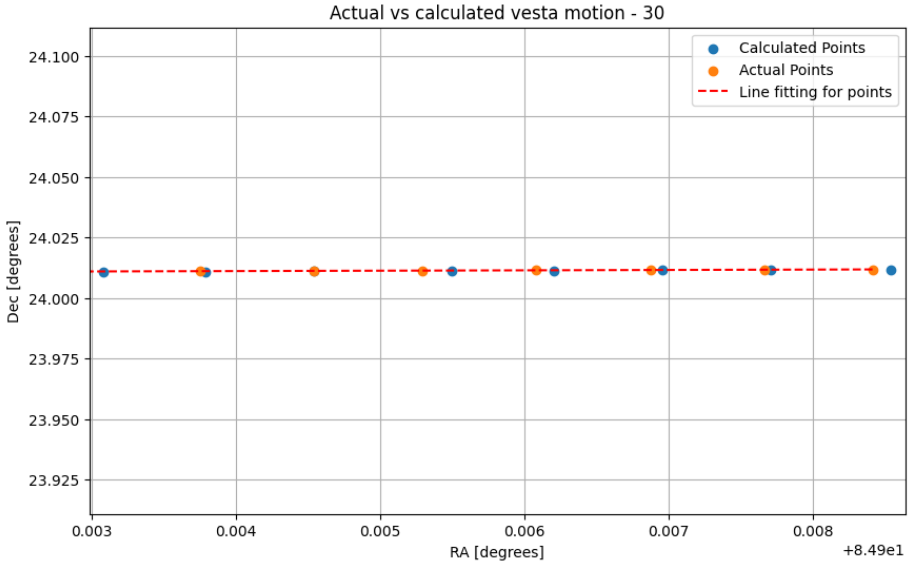

Figure 10: Comparison of calculated vs actual motion of Vesta for images of Exposure 30 seconds

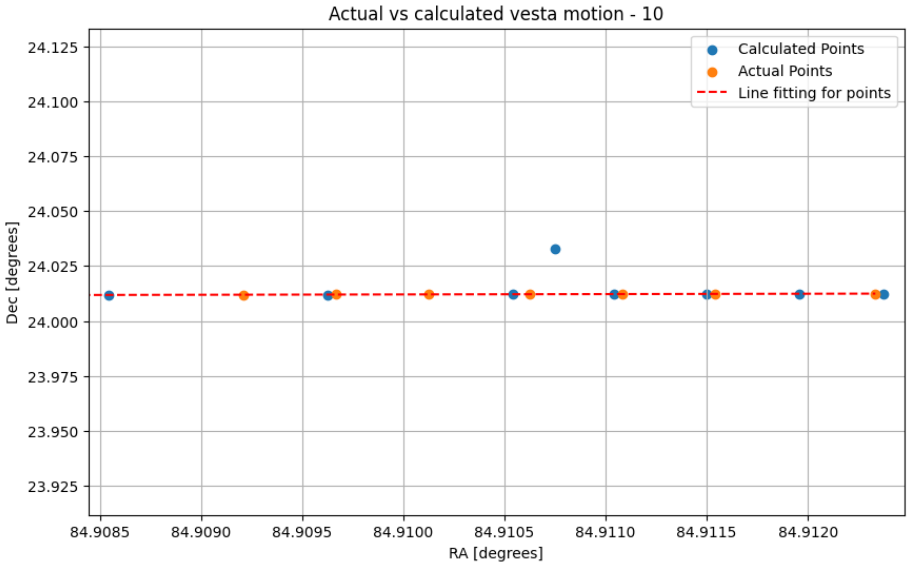

Figure 11: Comparison of calculated vs actual motion of Vesta for images of Exposure 10 seconds

6 Model Accuracy Analysis

6.1 Issues with our current work

6.1.1 Fixing CD Matrix with Astrometry.net

We have encountered significant issues when uploading FITS images directly to Astrometry.net; the CD matrices returned by the service are inaccurately calibrated. Despite our efforts to mitigate these inaccuracies, the results have been consistently imprecise. The following summarizes our findings for both 30-second and 10-second exposure times, with a particular focus on 'Web Astro' errors:

- **30 seconds exposure - Pixel Error (Web Astro):**
  - Median: 758,498.68
  - Standard Deviation: 4.55
- **10 seconds exposure - Pixel Error (Web Astro):**
  - Median: 759,549.86
  - Standard Deviation: 4.71
- **30 seconds exposure - RA/Dec Error (Web Astro):**

  - Median: 90,987.83
  - Standard Deviation: 334.15

- **10 seconds exposure - RA/Dec Error (Web Astro):**
  - Median: 91,144.82
  - Standard Deviation: 352.98

Although the outcomes of this investigation have not met our expectations, we still believe it essential to document our methodology, code, and insights within this report. This approach is undertaken in the hope that future work in this area may benefit from our preliminary efforts and potentially overcome the challenges we have faced. We acknowledge the inherent value of the method under consideration, despite our failure to implement it effectively within the allotted timeframe.

6.1.2 Inconsistency of GAIA star catalog usage

Due to the distributed nature of our project tasks, we encountered inconsistencies in the version of the Gaia star catalog used across different segments of our work. Specifically, while the majority of our codebase, including the error analysis components, utilized the Gaia DR2 (Data Release 2) as a reference, the manual calibration procedures were conducted with reference to the Gaia DR3 (Data Release 3). This discrepancy between Gaia catalog versions introduces a range of potential complications. Given that the Gaia catalogs are compiled at different times, there may be variations in stellar brightness and slight shifts in star positions over time. Consequently, this introduces an inadvertent bias against the manual calibration method, effectively penalizing it due to these inconsistencies, despite the possibility that its performance might not differ under uniform conditions. The mismatch in Gaia catalog versions undermines the comparability of our results, making it difficult to accurately assess the effectiveness of the manual calibration method against others within our study.

6.2 Decision to use Median and standard deviation for error analysis

In our error analysis, particularly when examining the relationship between flux and error, a critical consideration emerged regarding the variability of star brightness. As demonstrated in Figure 12, stars with flux values below 100 exhibit erratic behavior, which is a significant concern for our analysis.

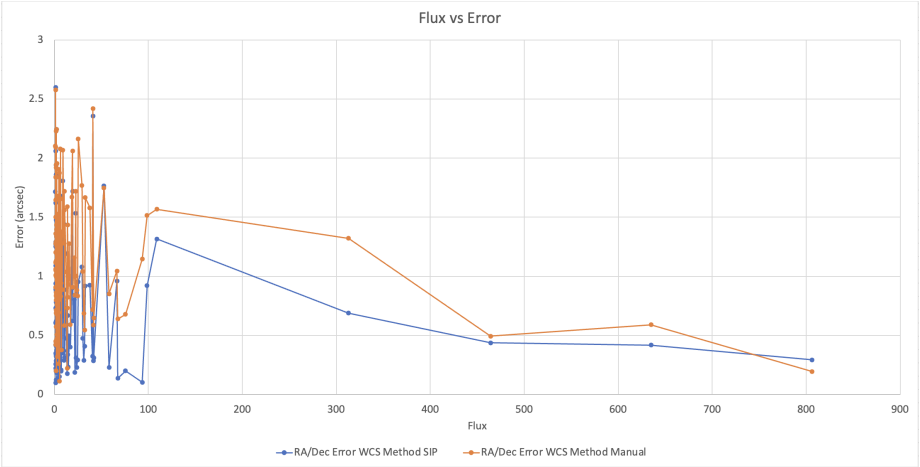

Figure 12: Flux versus error for vesta-0803-30.fit.

This observation aligns with the intuitive understanding that stars of lesser brightness are more susceptible to inaccuracies in measurement, thereby complicating the error analysis. Given this, the question is "How do we effectively evaluate our error metrics when the dataset is dominated by less bright stars, which are inherently more erratic?"

To address this challenge, we opted to utilize both the median and the standard deviation as our primary statistical measures. The mean, while commonly used, was deliberately excluded from our analysis due to its sensitivity to outliers, which could skew the results and provide a misleading representation of the data's central tendency. Nonetheless, relying solely on the median does not provide a complete picture of the data's distribution, especially concerning the variability within the dataset. Therefore, we also incorporated the standard deviation as a complementary measure.

By combining these two statistical tools, we aim to achieve a balanced and comprehensive analysis that accounts for both the central tendency and variability of the error measurements, thereby accommodating the diverse luminosity of the stars within our dataset.

6.3 Performance Analysis

For the performance analysis, we examine errors in pixels and Right Ascension and Declination (RA/Dec errors) relative to stars in the Gaia DR2 catalog. Our notation is as follows:

- `pixel_error_(Method_name)` for pixel errors,
- `ra_dec_error_(Method_name)` for RA/Dec errors.

The available method names are:

- **twirl**: Automated code using the Twirl library.
- **sip**: Automated code that queries through the Astrometry.net backend API, with SIP coefficients for distortion handling.
- **manual**: Manual calibration of the CD matrix method.

Refer to Table 1 for a detailed error analysis across various WCS methods for two different exposure times.

Table 1: Error analysis for various WCS methods across two exposure times.

Error Type	30s Median	30s Std Dev	10s Median	10s Std Dev
pixel_error_twirl	1.056479	4.860666	0.929249	5.895559
ra_dec_error_twirl	0.578493	2.590622	0.497890	2.652895
pixel_error_sip	1.650332	4.888599	1.823344	5.918842
ra_dec_error_sip	0.815720	2.598192	0.914262	2.692110
pixel_error_web_astro	758498.680137	4.550518	759549.862326	4.711171
ra_dec_error_web_astro	90987.832830	334.153471	91144.820817	351.984267
pixel_error_manual	2.807548	4.815796	3.279525	5.820705
ra_dec_error_manual	1.321982	2.582211	1.478529	2.675270

Figures 13 and 14 show the pixel and RA/Dec errors across all images, respectively.

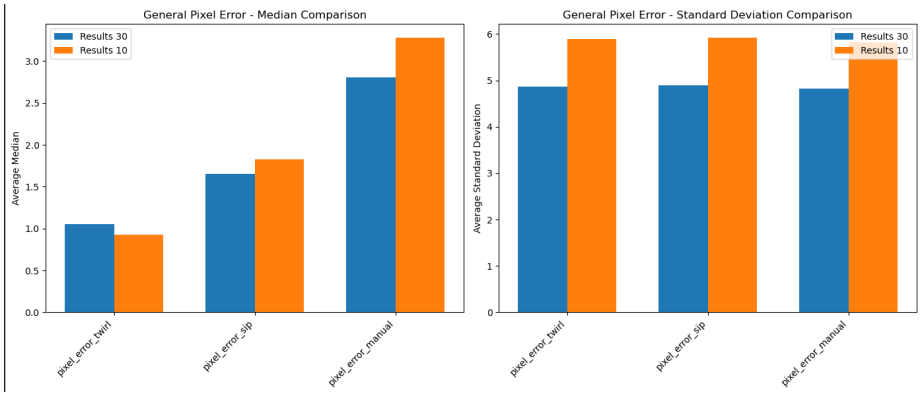

Figure 13: Pixel error across all images.

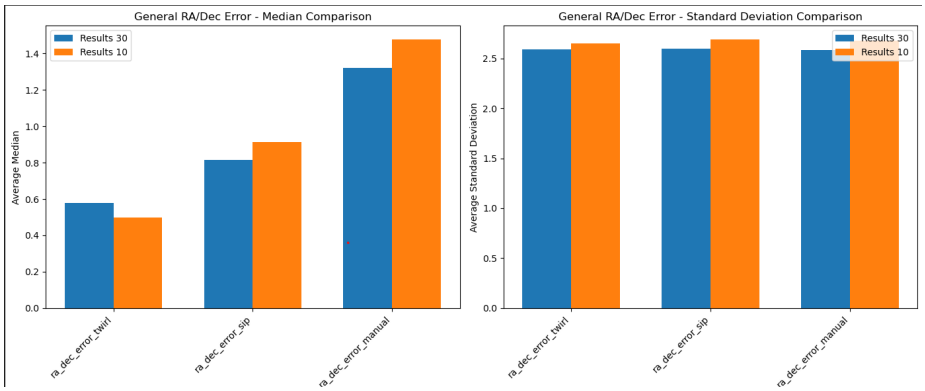

Figure 14: RA/Dec errors across all images.

The standard deviation figures across different methods and metrics show remarkable consistency. This uniformity suggests that the variation inherent in the methods, likely due to their shared use of DAOStarFinder, does not significantly impact the reliability of results from one run to the next.

For each specific model:

- **Twirl** performs the best, with a median error of around 0.58 arcsec. Interestingly, this method seems to perform better with lower exposure time, as the error increases with higher exposure time. This may be because Twirl, as a robust built-in library, encounters more margin for error with increased light.
- **SIP** performs second best, but the errors are still relatively high (0.91 arcsec for 10s and 0.81 arcsec for 30s). Unlike Twirl, SIP appears to react better with more exposure. This could be due to lens distortion being differently handled, and the algorithm might perform worse with the campus's lens compared to Twirl, which, to our knowledge, has no distortion handling.
- The **Manual** method performs the worst, with significantly higher error (above 2.5 arcsec). However, as previously mentioned, it is challenging to judge this method's validity due to the Gaia catalog mismatch. Nonetheless, we can deduce from the data that manual tuning of the CD matrix benefits from longer exposure images.

7 Discussion

This study detailed the precision achievable in localizing the asteroid Vesta using MTSU's 16" Schmidt-Cassegrain Telescope. Through a comparative analysis among automated (Astrometry.net and the twirl library), semi-automated (fixing CD matrix with Astrometry.net), and manual calibration in terms of

precision and accuracy. We have unearthed valuable insights into the capabilities and limitations of each method under both the 10-second and 30-second exposure times.

Manual and semi-automated methods showed significant efficiency and precision, aligning with the expectations for technological advancements in the field. They also provided invaluable checks against the automated methods, ensuring the reliability of the results obtained. These methods, especially with the precise determination of centroids for the brightest stars, demonstrated that traditional methods could still play a significant role in celestial cartography when used alongside modern automated techniques.

In contrast, the automated method, with Astrometry.net and the twirl library in particular, facilitated a straightforward and efficient calibration process in yielding accurate celestial coordinates with minimal error and an alternative means of calibration that closely matched the accuracy of corresponding celestial coordinates, further validating the robustness of automated calibration techniques.

Our analysis also examined the impact of exposure time on the precision of Vesta's localization. The results indicated that both 10-second and 30-second exposures provided sufficient accuracy for celestial cartography. However, the 30-second exposures, benefiting from a higher signal-to-noise ratio, demonstrated a slightly better alignment with the Gaia catalog positions, suggesting that longer exposures might be more beneficial for observations where high precision is critical.

8 Conclusion

Overall, this paper highlights the effect of manual, semi-automated (fixing CD matrix with Astrometry.net), and automated ((Astrometry.net and the twirl library)) calibration methods in determining the accurate location of celestial objects like Vesta. The automated calibration method provided a more consistent and user-friendly approach to celestial object localization, with SIP corrections further enhancing their accuracy. The manual and semi-automated calibration methods showed significant efficiency and precision and served as important comparative tools, underscoring the value of traditional techniques in verifying automated results. Furthermore, the findings suggest that incorporating longer exposures could enhance the precision of future observations, offering valuable insights for developing observational strategies.

References

[1] Developers, T. A. (n.d.). astropy: Astronomy and astrophysics core library. PyPI. Retrieved March 31, 2024, from https://pypi.org/project/astropy/

[2] World Coordinate System (astropy.wcs) — Astropy v5.0.1. (n.d.). Docs.astropy.org. https://docs.astropy.org/en/stable/wcs/index.html

[3] Astroquery — astroquery v0.4.7.dev2755. (n.d.). Astroquery.readthedocs.io. https://astroquery.readthedocs.io/en/latest/

[4] Garcia, L. J. (n.d.). twirl: Astrometric plate solving in Python. PyPI. https://pypi.org/project/twirl/

[5] Gaia Archive. (2020). Esa.int. https://gea.esac.esa.int/archive/

[6] Photutils — photutils 1.4.0. (n.d.). Photutils.readthedocs.io. https://photutils.readthedocs.io/en/stable/

[7] Astrometry.net. (n.d.). Astrometry.net. https://astrometry.net/

[8] Gary Bradski. *The OpenCV Library. Dr. Dobb's Journal of Software Tools*, 2000.